Sum-Frequency Spectroscopy of Molecular Adsorbates on Low-Index Ag Surfaces: Effects of Azimuthal Rotation

ARTICLE *in* ANALYTICAL CHEMISTRY · FEBRUARY 2009

Impact Factor: 5.64 · DOI: 10.1021/ac802332h · Source: PubMed

4 AUTHORS:

Scott K Shaw
University of Iowa
9 PUBLICATIONS **80** CITATIONS
SEE PROFILE

Alexei Lagutchev
Purdue University
44 PUBLICATIONS **720** CITATIONS
SEE PROFILE

Dana D Dlott
University of Illinois, Urbana-Champaign
297 PUBLICATIONS **6,640** CITATIONS
SEE PROFILE

Andrew A Gewirth
University of Illinois, Urbana-Champaign
207 PUBLICATIONS **5,575** CITATIONS
SEE PROFILE

Anal. Chem. **2009,** *81,* 1154–1161

Sum-Frequency Spectroscopy of Molecular Adsorbates on Low-Index Ag Surfaces: Effects of Azimuthal Rotation

Scott K. Shaw, Alexei Lagutchev, Dana D. Dlott,* and Andrew A. Gewirth*

School of Chemical Sciences, University of Illinois, 600 S. Mathews Avenue, Urbana, Illinois 61801

Vibrational sum-frequency generation spectroscopy (SFG) lineshapes of *p*-cyanobenzenethiol on low-index Ag crystal surfaces are studied as a function of azimuthal rotation by angle ϕ. A broadband multiplex SFG method is used, with a new technique that variably suppresses the nonresonant (NR) background using time-asymmetric time-delayed picosecond laser pulses. When both resonant (R) and NR signals are present, the amplitude and phase of the R line shape can vary significantly with ϕ, leading to dramatic ϕ-dependent variations of the SFG spectrum. The CN-stretch transition of *p*-cyanobenzenethiol modified Ag(111) and Ag(110) surfaces has an SFG spectrum consisting of a single vibrational resonance R atop a NR background that originates from the metal surface. Using the NR suppression technique, it was found that the R amplitude of the CN-stretch was independent of ϕ on both Ag(111) and Ag(110), which proves that the CN dipole moment is parallel to the surface normal in both cases. We show that it is possible to accurately extract the ϕ-dependence of the R amplitude, the NR amplitude, and the phase difference from SFG spectra by suppressing the NR signal during sample roation, thereby proving that the R contribution from the CN-stretch transition evidence ϕ-invariant behavior on both Ag surfaces.

This study examines vibrational sum-frequency generation spectroscopy[1−4] (SFG) of self-assembled monolayers (SAMs) of *p*-cyanobenzenthiol (CBT) on low-index Ag single-crystal substrates as a function of rotation around the surface normal by azimuthal angle ϕ. SFG has grown rapidly in popularity[5,6] because SFG provides high-quality vibrational spectra of surface and interfacial molecular species. SFG has proven especially valuable in the study of buried interfaces such as those found in electrochemical environments.[6−9] SFG is a nonlinear coherent spectroscopy in which an infrared (IR) pulse tuned near a vibrational resonance is combined with another pulse, conventionally called "visible" (in our measurements the "visible pulse" is actually 800 nm) to generate a coherent sum-frequency signal.[10] As with all nonlinear coherent spectroscopies such as coherent anti-Stokes Raman scattering,[11] the intensity, I, of SFG signals near a molecular resonance includes both a resonant (R) signal that depends on the IR frequency ω_{IR} and a non-resonant (NR) background which is largely independent of ω_{IR},

$$I_{SFG}(\omega_{IR},\phi) \propto |\chi^{(2)}_{NR}(\phi) + \chi^{(2)}_{R}(\omega_{IR},\phi)|^2 = |\chi^{(2)}_{NR}(\phi)|^2 + |\chi^{(2)}_{R}(\omega_{IR},\phi)|^2 + 2\cos(\psi(\phi))|\chi^{(2)}_{NR}(\phi)||\chi^{(2)}_{R}(\omega_{IR},\phi)| \quad (1)$$

where $\chi^{(2)}_{R}$ and $\chi^{(2)}_{NR}$ are the second-order susceptibilities.[10] The NR contribution can hinder analysis of the R signal because the NR signal is not simply an optical background. The SFG spectrum results from interference between the two contributions, characterized by a phase difference ψ (hereafter simply "the phase"). On single crystal substrates, the two susceptibilities and the phase depend on the azimuthal orientation angle ϕ, and the interplay among these factors can greatly complicate the analysis of orientation-dependent SFG spectra.

Azimuthal rotation reflection−absorption IR spectroscopy has been used to study the orientation of SAMs on single-crystal substrates,[12] specifically the polar angle θ between the molecular transition moment and the surface normal. Such measurements provide little information about the azimuthal orientation ϕ. SAMs typically exist in rotational domains that are much smaller than IR beam diameters of 200 μm or more.[13] The domains are related to each other by a rotation about the surface normal, and spectroscopic measurements sample a large number of equivalent domains.[14]

Owing to the successes of azimuthal rotation IR spectroscopy, it seems worthwhile to investigate azimuthal SFG methods. Second-harmonic generation (SHG), a special case of SFG, has been used extensively[15−28] to study the orientation dependence

* To whom correspondence should be addressed. E-mail: ddlott@illinois.edu (D.D.D.), agewirth@illinois.edu (A.A.G.). Phone: 217-333-3574 (D.D.D.), 217-333-8329 (A.A.G.). Fax: 217-244-3186 (D.D.D.), 217-244-3186 (A.A.G.).

(1) Eisenthal, K. B. *Chem. Rev. (Washington, D. C.)* **1996**, *96*, 1343.
(2) Shen, Y. R. *Nature* **1989**, *337*, 519.
(3) Shen, Y. R. *Appl. Phys. A: Solids Surf.* **1994**, *A59*, 541.
(4) Williams, C. T.; Beattie, D. A. *Surf. Sci.* **2001**, *500*, 545.
(5) Guyot-Sionnest, P. *Surf. Sci.* **2005**, *585*, 1.
(6) Smith, J. P.; Hinson-Smith, V. *Anal. Chem.* **2004**, *76*, 287A.
(7) Baldelli, S.; Gewirth, A. A. *Adv. Electrochem. Sci. Eng.* **2006**, *9*, 163.
(8) Shultz, M. J.; Schnitzer, C.; Simonelli, D.; Baldelli, S. *Int. Rev. Phys. Chem.* **2000**, *19*, 123.
(9) Tadjeddine, A. *Surf. Rev. Lett.* **2000**, *7*, 423.
(10) Shen, Y. R. *The Principles of Nonlinear Optics*; Wiley: New York, 1984.
(11) Eesley, G. L. *Coherent Raman Spectroscopy*; Pergamon: Oxford, 1991.
(12) Dubois, L. H.; Nuzzo, R. G. *Annu. Rev. Phys. Chem.* **1992**, *43*, 437.
(13) Siepmann, J. I.; McDonald, I. R. *Langmuir* **1993**, *9*, 2351.
(14) Yeganeh, M. S.; Dougal, S. M.; Polizzotti, R. S.; Rabinowitz, P. *Phys. Rev. Lett.* **1995**, *74*, 1811.
(15) Bilger, C.; Pettinger, B. *Chem. Phys. Lett.* **1998**, *294*, 425.
(16) Campbell, D. J.; Lynch, M. L.; Corn, R. M. *Langmuir* **1990**, *6*, 1656.
(17) Chen, C.-s.; Lue, J.-t.; Wu, C.-l.; Gwo, S.; Lo, K.-y. *J. Phys.: Condens. Matter* **2003**, *15*, 6537.

10.1021/ac802332h CCC: $40.75
Published on Web 12/30/2008

of NR signals from single crystals in wavelength ranges where only the NR signal is observed.[10] Azimuthal rotation of crystals with (111) surfaces gives NR signals having a $\cos^2(3\phi)$ intensity dependence, while rotation of (110) surfaces gives a $\cos^2(2\phi)$ intensity dependence.[28−32] The absolute value of the intensity is sensitive to environmental factors such as electrochemical potential and the dielectric constant of the contacting solvent.

Adsorbate structural information is accessed via the ϕ-dependence of the R molecular transitions. To study such effects, it is necessary to consistently and accurately extract the R amplitudes from ϕ-dependent SFG spectra. Unfortunately, the NR background varies significantly with ϕ. The analysis process becomes even more complicated if the phase ψ also varies with ϕ. In SFG studies of alkanethiol SAMs on Au(111), Yeganeh[14] et al. found that ψ does indeed have a ϕ-dependence, but the ϕ-dependence of the phase has not yet been studied in detail.

There are reasons to believe that the analysis of azimuthal rotation SFG spectra has not been done correctly in the past. In two existing prior studies of the ϕ-dependence of R amplitudes in SFG, which involved long-chain alkanethiols on Au(111) single-crystals[14] or Au(111) thin films oriented by oblique-angle vapor deposition,[33] researchers observed the expected $\cos^2(3\phi)$ NR intensity variations, but they also observed a surprising ϕ-dependence of the R amplitudes from CH-stretching transitions of the terminal methyl groups. There were pronounced deviations from the $\cos^2(3\phi)$ dependence that would be expected on the basis of the rotational symmetry of the SAM domains. Yeganeh[14] and co-workers concluded that octadecanethiol on Au(111) did not adsorb in the expected[12,34] $(\sqrt{3} \times \sqrt{3})$R30° structure but in fact formed an adlattice with a complicated mixed hollow and bridge site binding motif. Follonier and co-workers[33] interpreted the ϕ-dependence of the symmetric and asymmetric CH-stretch transitions of hexadecanethiol and pentadecanethiol on Au(111) as indicating that the angles θ between the surface normal and the C_{3v}-axis of the terminal methyl groups were 44° and 85° respectively, whereas conventional techniques such as diffraction or IR absorbance give[35] quite different tilt angles of 25° and 60°. So either these ϕ-dependent SFG measurements overturn conventional notions of SAM structures, or the process of extracting the ϕ-dependence of the R amplitudes was somehow flawed.

Recently there have been important advances in SFG technologies. In the works cited above, the SFG spectrometer used narrowband IR picosecond or nanosecond IR pulses which measured SFG spectra using point-by-point stepping. Many SFG spectrometers today use broadband femtosecond IR pulses in a multiplex configuration that allows an entire spectral region to be probed simultaneously.[36] In general this results in a great decrease in acquisition time and improved signal-to-noise ratios.

Quite recently the Dlott group has demonstrated an improved broadband SFG method that deeply suppresses the NR signal using time-delayed time-asymmetric visible pulses.[37] This technique requires only a simple modification of the usual broadband multiplex SFG apparatus, replacing the more typical visible frequency-filtering devices (zero-dispersion monochromators or interference filters) with a Fabry−Perot étalon, allowing the R signal to be studied in the absence of the NR background even on metal surfaces where the NR is usually quite large. As we show here, this technique totally obviates the need for complicated data analysis in ϕ-dependent SFG measurements.

For a critical test of our ability to determine the ϕ-dependence of SFG R amplitudes, we chose to study CBT modified surfaces. CBT on Au(111) forms a SAM where the CN moieties are oriented nearly upright[38] ($\theta = 0°$), and we expect this to be the case on Ag(111) and possibly on Ag(110) based on similarities between SAMs formed on the different surfaces.[39−41] With adsorbates that have a significant tilt, such as the alkanethiols, the R amplitudes should have a strong $\cos^2(n\phi)$ dependence, and we would have to determine whether or not other Fourier components are present in the data. For example on Ag(111) there would be a large $\cos^2(3\phi)$ dependence, and we would have to test for the presence of minor components of $\cos^2(2\phi)$, $\cos^2(4\phi)$, and so forth, which would be difficult. With upright molecules the R amplitudes would be independent of azimuthal rotation,[42,43] so if we obtained a ϕ-invariant signal we could be confident of our results.

However, it is also important and useful to be able to extract R amplitudes when the NR signal is present. The relative phase of the R and NR contributions cannot be measured when the NR is suppressed, but the phase provides useful information about interactions between the surface and its environment and can be

(18) Corn, R. M.; Higgins, D. A. *Chem. Rev.* **1994**, *94*, 107.
(19) Horswell, S. L.; Pinheiro, A. L. N.; Savinova, E. R.; Danckwerts, M.; Pettinger, B.; Zei, M.-S.; Ertl, G. *Langmuir* **2004**, *20*, 10970.
(20) Ito, F.; Hirayama, H. *Phys. Rev. B: Condens. Matter Mater. Phys.* **1994**, *50*, 11208.
(21) Lynch, M. L.; Barner, B. J.; Corn, R. M. *J. Electroanal. Chem. Interfacial Electrochem.* **1991**, *300*, 447.
(22) Lynch, M. L.; Corn, R. M. *J. Phys. Chem.* **1990**, *94*, 4382.
(23) Pettinger, B.; Bilger, C. *Chem. Phys. Lett.* **1998**, *286*, 355.
(24) Yamada, C.; Kimura, T. *Phys. Rev. B: Condens. Matter Mater. Phys.* **1994**, *49*, 14372.
(25) Yagi, I.; Chiba, M.; Uosaki, K. *J. Am. Chem. Soc.* **2005**, *127*, 12743.
(26) Yagi, I.; Nakabayashi, S.; Uosaki, K. *Journal of Physical Chemistry B* **1998**, *102*, 2677.
(27) Daschbach, J. L.; Fischer, P. R.; Gragson, D. E.; Richmond, G. L. *J. Phys. Chem.* **1995**, *99*, 3240.
(28) Georgiadis, R.; Richmond, G. L. *J. Phys. Chem.* **1991**, *95*, 2895.
(29) Mitchell, S. A.; Boukherroub, R.; Anderson, S. *J. Phys. Chem. B* **2000**, *104*, 7668.
(30) Pettinger, B.; Danckwerts, M.; Krischer, K. *Faraday Discuss.* **2002**, *121*, 153.
(31) Fomenko, V.; Bodlaki, D.; Faler, C.; Borguet, E. *J. Chem. Phys.* **2002**, *116*, 6745.
(32) Bourguignon, B.; Zheng, W.; Carrez, S.; Fournier, F.; Gaillard, M. L.; Dubost, H. *Surf. Sci.* **2002**, *515*, 567.
(33) Follonier, S.; Miller, W. J. W.; Abbott, N. L.; Knoesen, A. *Langmuir* **2003**, *19*, 10501.
(34) Schreiber, F. *Prog. Surf. Sci.* **2000**, *65*, 151.
(35) Laibinis, P. E.; Whitesides, G. M.; Allara, D. L.; Tao, Y. T.; An, P.; Nuzzo, R. G. *J. Am. Chem. Soc.* **1991**, *113*, 7152.
(36) Richter, L. J.; Petralli-Mallow, T. P.; Stephenson, J. C. *Opt. Lett.* **1998**, *23*, 1594.
(37) Lagutchev, A.; Hambir, S. A.; Dlott, D. D. *J. Phys. Chem. C* **2007**, *111*, 13645.
(38) Hallmann, L.; Bashir, A.; Strunskus, T.; Adelung, R.; Staemmler, V.; Woll, C.; Tuczek, F. *Langmuir* **2008**, *24*, 5726.
(39) Laibinis, P. E.; Bain, C. D.; Nuzzo, R. G.; Whitesides, G. M. *J. Phys. Chem.* **1995**, *99*, 7663.
(40) Laibinis, P. E.; Whitesides, G. M.; Allara, D. L.; Tao, Y. T.; Parikh, A. N.; Nuzzo, R. G. *J. Am. Chem. Soc.* **1991**, *113*, 7152.
(41) Nuzzo, R. G.; Dubois, L. H. *Surf. Sci.* **1985**, *149*, 119.
(42) Hirose, C.; Akamatsu, N.; Domen, K. *J. Chem. Phys.* **1992**, *96*, 997.
(43) Hirose, C.; Akamatsu, N.; Domen, K. *Appl. Spectrosc.* **1992**, *46*, 1051.

used to deduce the absolute molecular orientation[1,44] or to monitor the dynamic potential-dependent reorientation[9,45,46] of molecules in electrochemical environments. For this reason we have also measured ϕ-dependent SFG spectra of CBT on low-index Ag crystal surfaces under conditions where the NR contribution is at a maximum to determine whether we can accurately extract the dependence of R amplitudes on azimuthal rotation.

SFG Spectroscopy. SFG spectra were originally acquired by combining fixed-frequency narrow-band visible pulses and tunable narrow-band IR pulses.[2] The IR pulses were stepped through vibrational resonances while the SFG total intensity was monitored. In the broadband multiplex configuration, a femtosecond IR pulse having a range of IR frequencies is combined with a fixed-frequency narrow-band picosecond visible pulse while a spectrograph and array detector spectrally resolve the SFG signal.

As discussed in the introduction, the SFG signal results from the square of the sum of the R and NR amplitudes. The NR background is most significant for molecules adsorbed on metal substrates,[7,8,47,48] especially Au, Ag, and Cu. The NR phase and intensity depend significantly on the wavelength of the visible pulses[47] but very little on the IR pulse wavelength, so NR signals generally appear as a frequency-independent background beneath the vibrational resonances. The NR intensity and phase may depend on many factors: angle of incidence,[49] applied electrochemical potential,[7] solvent refractive index,[50] orientation of single-crystal axes or of partially ordered single-crystal domains with respect to incident radiation,[14] and temporal overlap of incident laser pulses.[37]

Azimuthal rotation can strongly affect the NR amplitude, so to illustrate some of the issues that result, we consider a well-known model system: the SFG spectrum from a single vibrational resonance represented by a Lorentz line shape centered at frequency ω_0 against a frequency-independent NR background. The SFG spectrum then takes the form,[51]

$$I_{SFG}(\omega_{IR}+\omega_{vis},\phi) \propto \left|\chi^{(2)}_{NR}(\phi)+\frac{A(\phi)e^{i\psi(\phi)}}{\omega_{IR}-\omega_0+i\Gamma}\right|^2 = |\chi^{(2)}_{NR}(\phi)|^2 + |\chi^{(2)}_{R}(\phi)|^2 + 2|\chi^{(2)}_{NR}(\phi)||\chi^{(2)}_{R}(\phi)|\cos\psi(\phi) \quad (2)$$

where $A(\phi)$ is the parameter that determines the ϕ-dependence of the R amplitude, ω_0 is the vibrational transition center frequency, Γ is the line width (damping parameter), and $\psi(\phi)$ the phase.

In broadband multiplex SFG, the spectrum is modified by the distribution of IR wavelengths in the femtosecond pulse, similar to the way point-by-point scans must be normalized by the variation in IR pulse intensity during the scan. We will approximate

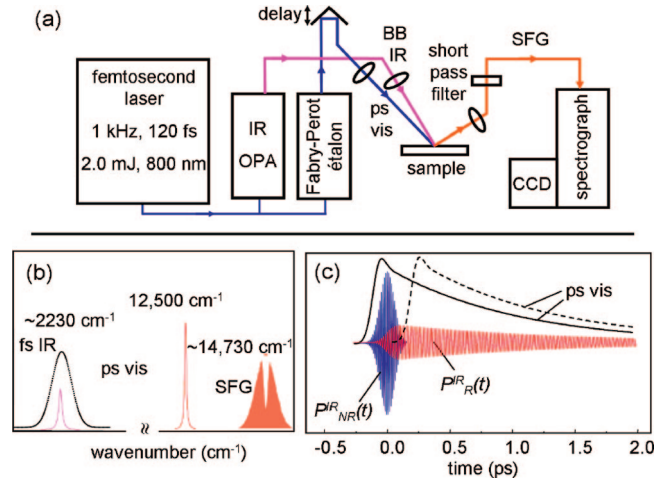

Figure 1. (a) Block diagram of the laser apparatus. Part of the femtosecond pulse is used to generate a broadband femtosecond IR pulse (BBIR) in an optical parametric amplifier (OPA), and part is used to generate a time-asymmetric picosecond visible pulse in an étalon.[65] (b) Broadband multiplex scheme. All vibrational transitions that overlap the femtosecond IR pulse spectrum generate SFG signals monitored using a multichannel spectrograph. (c) Time domain picture. The femtosecond IR pulses create a polarization consisting of a R part $P^{IR}_{R}(t)$ and a NR part $P^{IR}_{NR}(t)$. The time-asymmetric picosecond visible pulses interact with the polarizations to generate SFG signals. The NR part originating from the metal surface has a faster response that tracks the femtosecond IR pulse temporal envelope. The R part originating from molecular vibrations persists for a longer time on the order of T_2. A time-delayed picosecond visible pulse (dashed curve) suppresses the NR contribution.

the pulse spectrum as a Gaussian centered at laser frequency ω^L_{IR} with spectral width $\delta\omega_L$,[52,53] ($\delta\omega_L$ is typically 200−250 cm^{-1}),

$$I_{SFG}(\omega_{IR}+\omega_{vis},\phi) \propto e^{\left[\frac{(\omega-\omega^L_{IR})^2}{2(\delta\omega_L)^2}\right]}\left|\chi^{(2)}_{NR}(\phi)+\frac{A(\phi)e^{i\psi(\phi)}}{\omega-\omega_0+i\Gamma}\right|^2 \quad (3)$$

The experimental arrangement[37] used for broadband multiplex SFG is depicted schematically in Figure 1a. A 120 fs duration laser pulse from an amplified Ti:sapphire laser at 800 nm is split into two parts. One part generates the femtosecond IR using an optical parametric amplifier with a difference-frequency generation stage. The second part generates the picosecond visible pulses after transmission through an air-spaced Fabry−Perot étalon. The round-trip time in the air gap is less than the pulse duration. When the femtosecond pulse is incident on this type of étalon, the transmitted output pulse has a time-asymmetric profile consisting of a faster femtosecond rising edge and a slower picosecond decay that is determined by the ring-down time of the étalon cavity.[37] The output pulse is a narrow band of visible light centered near 800 nm, having an approximately Lorentzian spectrum.

Figure 1b depicts the broadband multiplex SFG concept in the frequency domain. The femtosecond IR pulse spectrum determines which vibrational transitions will contribute to the signal. The picosecond visible pulse spectrum determines the overall

(44) Kemnitz, K.; Bhattacharyya, K.; Hicks, J. M.; Pinto, G. R.; Eisenthal, K. B.; Heintz, T. F. *Chem. Phys. Lett.* **1986**, *131*, 285.
(45) Baldelli, S.; Mailhot, G.; Ross, P.; Shen, Y. R.; Somorjai, G. A. *J. Phys. Chem. B* **2001**, *105*, 654.
(46) Shaw, S. K.; Lagutchev, A.; Dlott, D. D.; Gewirth, A. A. *J. Phys. Chem.* **2008**, accepted for publication.
(47) Potterton, E. A.; Bain, C. D. *J. Electroanal. Chem.* **1996**, *409*, 109.
(48) Matranga, C.; Wehrenberg, B. L.; Guyot-Sionnest, P. *J. Phys. Chem. B* **2002**, *106*, 8172.
(49) Tadjeddine, A.; Guyot-Sionnest, P. *J. Phys. Chem.* **1990**, *94*, 5193.
(50) Schultz, Z. D.; Shaw, S. K.; Gewirth, A. A. *J. Am. Chem. Soc.* **2005**, *127*, 15916.
(51) Superfine, R.; Huang, J. Y.; Shen, Y. R. *Phys. Rev. Lett.* **1991**, *66*, 1066.
(52) Lagutchev, A.; Lu, G. Q.; Takeshita, T.; Dlott, D. D.; Wieckowski, A. *J. Chem. Phys.* **2006**, *125*, 154705.
(53) Lu, G. Q.; Lagutchev, A.; Dlott, D. D.; Wieckowski, A. *Surf. Sci.* **2005**, *585*, 3.
(54) Wang, Z.; Carter, J. A.; Lagutchev, A.; Koh, Y. K.; Seong, N.-H.; Cahill, D. G.; Dlott, D. D. *Science* **2007**, *317*, 787.

spectral resolution, here 10.3 cm^{-1}, since the spectrograph has resolving power greater than 10.3 cm^{-1}.[37]

To understand the NR suppression technique, we must describe the SFG process in the time domain.[37,54] The combined IR−Raman interaction in the dipole approximation is characterized by the hyperpolarizability correlation function

$$C(t) = \langle \mu(t)\alpha(0) \rangle \quad (4)$$

where μ represents the dipole moment and α the polarizability tensor.[55] The ensemble-average hyperpolarizability yields the second-order susceptibility $\chi^{(2)}$ in eqs 1−3.[10] The SFG spectrum is related to the Fourier transform of eq 4, which shows that SFG process can be viewed as an IR excitation via μ and a coherent Raman process via α.[55] As depicted in Figure 1c, a femtosecond IR pulse creates a coherent polarization (ensemble-averaged dipole) in the medium that oscillates at frequencies near ω_{IR}. The polarization can be separated into two parts, $P^{IR}_{NR}(t)$ and $P^{IR}_{R}(t)$. These polarizations undergo free-induction decays. The $P^{IR}_{NR}(t)$ part, originating from electronic transitions of the metal surface, responds so rapidly that its decay mirrors the femtosecond IR pulse duration of ~200 fs. The $P^{IR}_{R}(t)$ part, originating from molecular vibrations resonant with the femtosecond IR pulse, decays with a time constant $T_2 = (\pi c \Delta\nu)^{-1}$ where $\Delta\nu$ is the vibrational line width, and c the speed of light. T_2 is typically in the 1 ps range, for example, when $\Delta\nu = 10$ cm^{-1}, $T_2 = 1.06$ ps. This disparity in time scales, ~200 fs for the NR part and ~1 ps for the R part, allows us to suppress the NR signal by time windowing.[37] When the picosecond visible pulse is incident on the sample while $P^{IR}(t)$ is nonzero, a sum signal is generated by a coherent anti-Stokes Raman scattering process. Thus (in the dipole approximation) the only vibrations that contribute to the SFG signal are those that are simultaneously IR and Raman active.[2] Because the picosecond visible pulse has a time-asymmetric profile, it can be time-delayed to a point where its rising edge lies just beyond $P^{IR}_{NR}(t)$ (Figure 1c), while still interacting with an appreciable part of $P^{IR}_{R}(t)$. In this case the generated SFG signal has the NR part deeply suppressed while the R part is only slightly suppressed.

To better understand the SFG spectra obtained in measurements where the NR and phase vary significantly because of azimuthal rotation, and to understand the significance of the NR suppression technique, we have simulated some representative SFG lineshapes using eq 2, as described in ref 56. Figure 2a shows the purely R contribution, a Lorentz line given an amplitude of unity and fwhm of 10 cm^{-1}. In subsequent Figures 2(b−l), the NR amplitude is set equal to the R amplitude and only the phase ψ is varied. When the NR and R signals are in phase ($\psi = 0$), the NR background can significantly increase the R signal intensity by the heterodyne effect, since the R signal derives from two terms, $|\chi^{(2)}_R|^2$ and $2|\chi^{(2)}_{NR}||\chi^{(2)}_R|$. Thus, in Figure 2b the R contribution appears as a peak having three times the intensity of the NR background. The peak is no longer a Lorentzian, since it is the sum of a Lorentz function and the square of a Lorentz function. In Figure 2c the R signal is out-of-phase with $\psi = -\pi$, so the resonance appears as a Lorentzian dip in the background. In

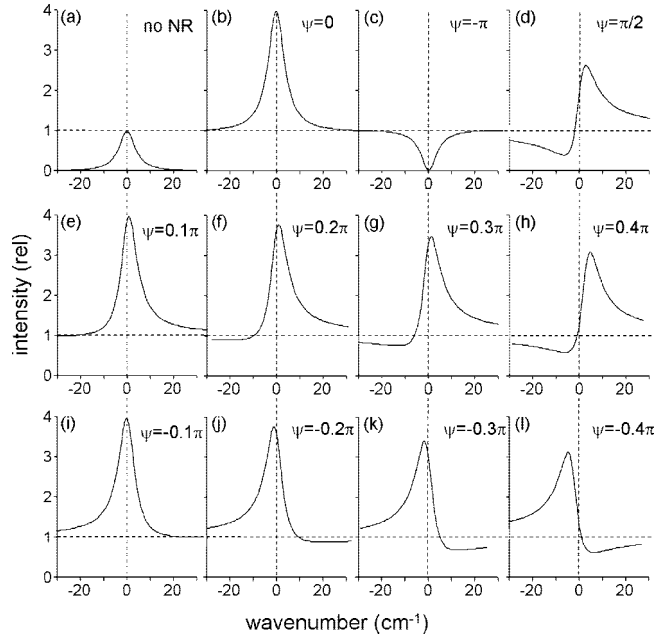

Figure 2. Simulated SFG spectra computed using eq 2. (a) In the absence of a NR contribution, the R contribution is a Lorentzian with unit intensity and fwhm of 10 cm^{-1}. All subsequent panels have NR and R amplitudes equal to unity, but the phase ψ (rad) is varied as indicated.

Figure 1d, the R signal has $\psi = \pi/2$, and the resonance has a derivative shape. The derivative shape occurs because the phase of a Lorentz oscillator has the well-known form[56] $\phi(\omega) = (\omega - \omega_0)/(\omega - \omega_0 + i\Gamma)$. In Figures 1(e−l), the phase ψ is varied from -0.4π to 0.4π. These phase angles affect the peak intensity and result in asymmetries and peak shifts.

If different laboratories obtained SFG spectra of a particular transition of a molecular adsorbate on a metal surface, they would all use the same IR wavelengths but might not use the same visible wavelength. Since the phase ψ can vary with ω_{vis}, SFG spectra of the same sample could appear entirely different. For example, some SFG spectra of alkanethiols on Ag feature methyl bands that appear derivative-shaped while some appear as peaks[47] and others as dips.[36]

When SFG spectra are analyzed in a quantitative manner,[53,57,58] it is usually by fitting to eq 2, or a simple modification of eq 2 that treats the R term as a sum of multiple Lorentz resonances. In the fitting process the adjustable parameters are the R and NR amplitudes, ω_0 and Γ, and the phase angle ψ. The phase angle is frequently problematic. It is always difficult to determine fitting parameters that are strongly coupled, and as seen in Figure 2, changing the phase can have a major effect on the amplitude and some effect on the peak frequency as well. Extracting the correct phase is ordinarily predicated on the a priori assumption of a Lorentz line shape. But actual vibrational lineshapes need not be Lorentzian, and if this were the case it would surely affect the NR and phase determinations. The theory of vibrational lineshapes for ordered or disordered molecular

(55) Shen, Y. R. *Surf. Sci.* **1994**, *299/300*, 551.
(56) Ward, R. N.; Davies, P. B.; Bain, C. D. *J. Phys. Chem.* **1993**, *97*, 7141.
(57) Wang, H.-F.; Gan, W.; Lu, R.; Rao, Y.; Wu, B.-H. *Int. Rev. Phys. Chem.* **2005**, *24*, 191.
(58) Wang, J.; Clarke, M. L.; Chen, Z. *Anal. Chem.* **2004**, *76*, 2159.

assemblies[59−61] is well developed and will not be discussed in detail here, but we note the possibility of inhomogeneous broadening which ordinarily yields a Voight rather than a Lorentz line shape.[62] Inhomogeneous broadening can result from sample inhomogeneities and thermal fluctuations in the molecular adlattice structure or the populations of lower-energy vibrations.

Equation 2 and Figure 2 also illustrate the difficulties that might be encountered in trying to determine the molecular coverage N in SFG single-crystal studies. Depending on the relative R and NR contributions, the SFG signal intensity might range from linearly proportional to N (when NR ≫ R) to quadratic in N (when R ≫ NR). In the NR suppression technique, the R intensity is always quadratic in N.

EXPERIMENTAL SECTION

Sample Preparation. Ag(111) and Ag(110) single crystals were obtained from Monocrystals Co., Medina, OH. Crystal orientation was determined to better than 1° using Laue X-ray backscattering. The crystal was mechanically polished to a mirror finish using progressively finer grit Al_2O_3 or diamond paste (Buehler Consumables) ending with 0.3 or 0.25 μm grit size, respectively, and finally cleaned in a chemical etch using a hexavalent chromium solution[63] before being placed under Milli-Q water (18.2 MΩ cm) to protect the surface until use.

The CBT was synthesized as previously described.[64]^{1}H NMR, FTIR, and mass spectrometry confirmed the synthesis. Monolayers of CBT were formed on Ag surface by immersing the crystal in a 1 mM CBT in ethanol solution for at least 24 h. After deposition, samples were stored in the dark in the CBT solution to maintain surface quality until use. All spectra were acquired ex-situ under ambient conditions. Initial azimuthal alignment was achieved by scoring a mark on the crystal edge along the (011) or (100) axes—found by using X-ray reflectivity—on the Ag(111) and Ag(110) single crystals, respectively. At the beginning of each experiment, the marked axes were oriented vertically on the sample stage (or perpendicular in relation to the direction of incident light waves) defining a zero of rotation. For the (111) sample, this configuration aligned the $\bar{2}11$ axis parallel to the incident light at zero degrees rotation as the light travels from left to right. For the (110) sample, the configuration aligned the $\bar{1}10$ axis parallel to the incident light at zero degrees rotation.

The crystals were fixed to an azimuthal rotation stage and a special kinematic mount. The SFG spectrometer is prealigned for surfaces in a reference plane. The kinematic mount allowed us to tilt the crystals and translate them in the z-direction (normal to the plane) to align their surfaces with the reference plane. There is also the capability of translating along xy directions (in the plane) to avoid blemishes or imperfections. To accomplish these tasks, the kinematic mount consisted of a combination of xyz translation stages and a two-axis goniometer.

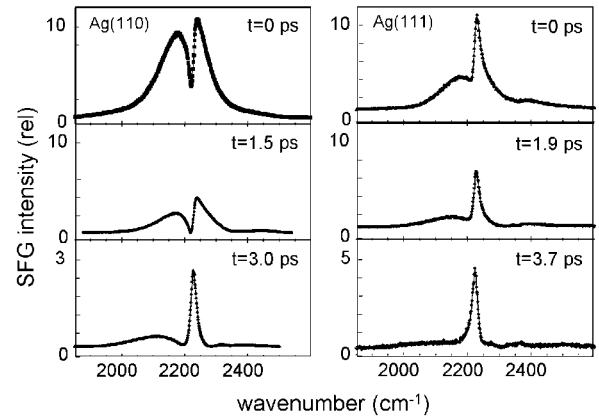

Figure 3. SFG spectra acquired from CBT-modified Ag(110) and Ag(111) single crystal surfaces ($\phi = 0°$) as a function of time delay of the time-asymmetric picosecond visible pulses. Time zero denotes the time delay when the NR signal is a maximum. As the picosecond visible pulse is delayed, the NR contribution is suppressed. The NR signal remaining in the Ag(110) data at $t = 3$ ps is due to laser pulse distortion created via high-intensity propagation through a window. This effect was greatly decreased in the Ag(111) measurements.

SFG Spectra. The Ti:sapphire laser (Quantronix Integra-C 2.0) produced 2.0 mJ pulses of 120 fs duration at 800 nm at a repetition rate of 1 kHz.[37] Three-quarters of each pulse pumped an IR OPA (Light Conversion TOPAS-C 800 fs DFG). One-fourth of each pulse was filtered by an étalon (TecOptics) with air gap $d = 11.1$ μm, free-spectral range = 450 cm^{-1}, and finesse = 44 to produce a time-asymmetric picosecond pulse with spectral bandwidth $\Delta\nu = 10.3$ cm^{-1}. At the sample the IR pulse centered near 2230 cm^{-1} had an energy of ∼5 μJ and the $(1/e^2)$ beam diameter was 200 μm. The visible pulse energy was ∼20 μJ and the beam diameter was 300 μm. The incidence angles were close to 60° All spectra were obtained in the ppp polarization condition. Delay between the IR and visible pulses was generated by using a delay line actuated by a stepper motor.[37] The delay time is given relative to a time denoted zero where the NR signal intensity was a maximum. The coherent SFG signal beam was focused into a spectrograph (Andor Shamrock) with a CCD detector. Each spectrum was obtained with an acquisition time of 10s.

RESULTS

SFG with NR Background Suppression. Figure 3 shows SFG spectra of CBT-modified Ag(110) and Ag(111) where the azimuthal rotation was fixed at $\phi = 0$ but the time delays between the femtosecond IR pulses and the time-asymmetric picosecond visible pulses were varied. On the Ag(110) surface at $t = 0$ the resonance feature appears as a dip. On the Ag(111) surface with $t = 0$, it is a peak. But whether the CBT resonance originally appeared as a peak or as a dip, the NR background declined with increasing delay until the R feature appeared as a peak only. Figure 4 characterizes how the NR intensity decreases with increasing time delay. At >3 ps delay, the NR signal is negligible and the R signal intensity remains substantial. Notice that in the Ag(110) data the NR signal to the low energy side of the CBT resonance is not entirely suppressed because of laser pulse chirp.

(59) Chronister, E. L.; Dlott, D. D. *J. Chem. Phys.* **1983**, *79*, 5286.
(60) Velsko, S.; Hochstrasser, R. M. *J. Phys. Chem.* **1985**, *89*, 2240.
(61) Decola, P. L.; Hochstrasser, R. M.; Trommsdorff, H. P. *Chem. Phys. Lett.* **1980**, *72*, 1.
(62) Kubo, R.; Tomita, K. *J. Phys. Soc. Jpn.* **1954**, *9*, 888.
(63) Smolinski, S.; Zelenay, P.; Sobkowski, J. *J. Electroanal. Chem.* **1998**, *442*, 41.
(64) Seed, A. J.; Toyne, K. J.; Goodby, J. W.; McDonnell, D. G. *J. Mater. Chem.* **1995**, *5*, 1.
(65) Carter Jeffrey, A.; Wang, Z.; Dlott Dana, D. *J. Phys. Chem. A* **2008**, *112*, 3523.

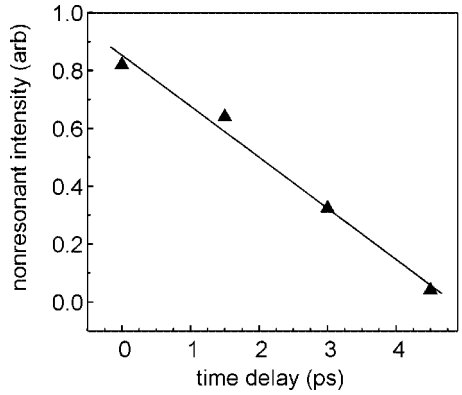

Figure 4. NR signal intensity from bare Ag(111) surface as a function of time delay showing how the NR contribution can be deeply suppressed by time delays >3 ps.

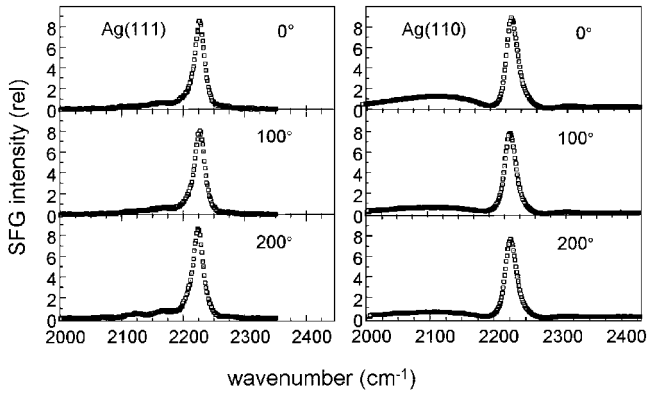

Figure 5. Azimuthal-angle-dependent SFG spectra from CBT on Ag(111) and Ag(110) with the NR contribution suppressed by time delay.

It turned out that the IR spectrum from the OPA was not a perfect Gaussian as described by eq 3. The central spectrum was a good fit to a Gaussian, but there were tails on the red and blue edges and sometimes a second peak on the blue edge, which varied from day to day. After the Ag(110) experiments were concluded, it was found that these spectral distortions were the result of frequency chirping of the Ti:sapphire pulses as they passed through a too-thick window in the exit port of the laser, which were then transferred to the IR pulses. The chirp effect creates new frequencies that have an extended temporal structure. In the subsequent Ag(111) measurements the system was adjusted to greatly reduce this chirp effect.

Some representative SFG spectra obtained with NR suppression as a function of azimuthal orientation are shown in Figure 5. In Figure 6 we plot the ϕ-dependence of the CN-stretch R amplitude on both Ag(110) and Ag(110) surfaces. The R amplitude is the square root of the peak intensity. On both Ag surfaces the R amplitudes are, within experimental error, independent of ϕ. The error bars on these measurements, that is, the differences in values obtained by taking spectra repeatedly, were smaller than the data points themselves. The largest source of error was systematic error due to laser beam alignment. We could not align the sample surface so that the laser beams were precisely on the axis of rotation, so that as the sample was rotated, the beams wandered slightly over the crystal surface. The small variations

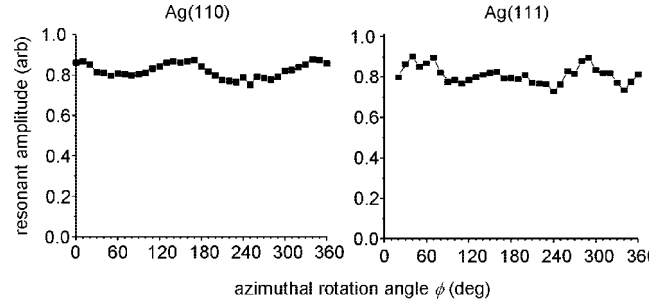

Figure 6. Azimuthal angle dependence of the R amplitude of the CN-stretch transition of CBT on Ag(110) and Ag(111) when NR suppression is used. On both crystal surfaces the CN-stretch R amplitude is independent of azimuthal angle ϕ.

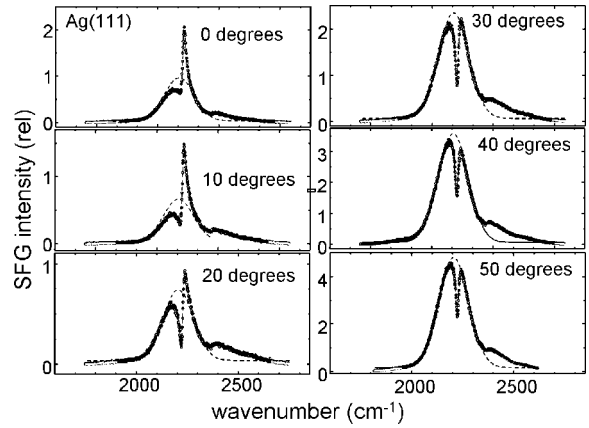

Figure 7. SFG spectra obtained from Ag(111) single crystal surface modified with CBT monolayer, with azimuthal rotation about angle ϕ as indicated. Open symbols are experimental data, solid curves are best fits to eq 3, and the dashed lines indicate the idealized Gaussian spectrum of the femtosecond IR pulses. The actual pulse spectra deviate from a Gaussian in the wings, which does not affect the data analysis.

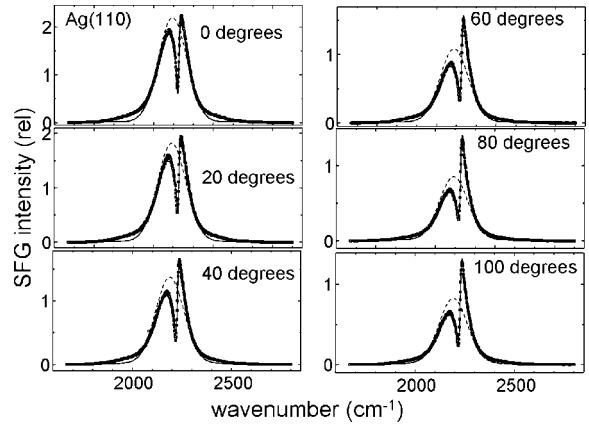

Figure 8. SFG spectra obtained from Ag(110) single crystal surface modified with CBT, with azimuthal rotation about an angle ϕ as indicated. Open symbols are experimental data, solid curve is the best fit to eq 3, and the dashed lines indicate the idealized Gaussian spectrum of the femtosecond IR pulses.

in the amplitudes seen in Figure 6 are attributed to these systematic errors.

SFG with NR Background. The SFG data in Figures 7−11 were obtained with the IR-visible delay set to time zero. Figure 7

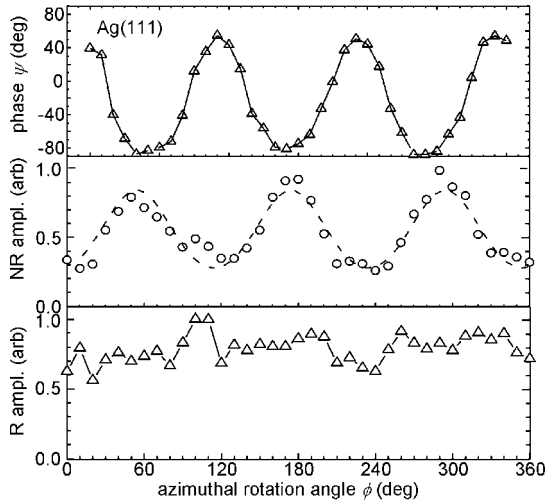

Figure 9. Parameters extracted by fitting the Ag(111) CBT spectra from Figure 7 using eq 3. Top: phase difference ψ between the R CN-stretch transition and the NR background. The solid curve is a fit to eq 5 with 3-fold symmetry. Middle: NR amplitude. The dashed curve is a fit to eq 5. Lower: R amplitude.

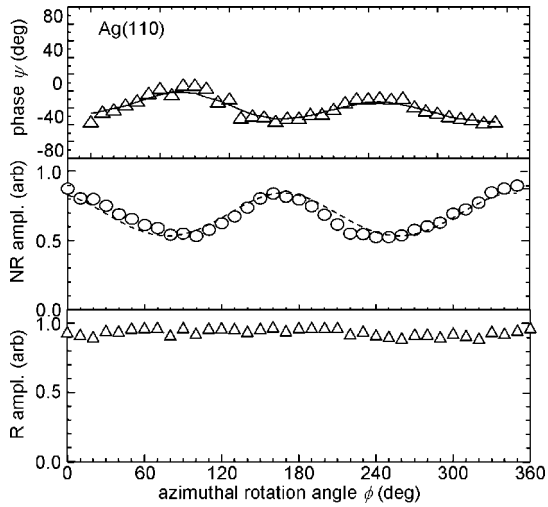

Figure 10. Parameters extracted by fitting the Ag(110) CBT spectra from Figure 8 using eq 3. Top: phase difference ψ between the R CN-stretch transition and the NR background. The solid curve is a fit to eq 5 with 2-fold symmetry. Middle: NR amplitude. The dashed curve is a fit to eq 5. Lower: R amplitude.

and 8 show SFG spectra in the CN-stretch region of CBT-modified Ag(111) or Ag(110) surfaces. The SFG spectra of CBT on Ag(100) surface (not shown) exhibited little orientational dependence, as expected from the isotropic surface nonlinear susceptibility tensor for 4-fold symmetry,[19,47] and from previous SHG measurements.[19]

In Figures 7 and 8 the spectra have a single resonance near 2230 cm^{-1} due to the CN-stretch of CBT plus a NR background which, as described by eq 3, mimics the spectrum of the femtosecond IR pulses. The IR pulses were tuned so that the resonance appeared near the flat part at the spectral peak, which maximized the R intensity and made the fitting procedure most accurate. To emphasize the Gaussian NR component, all the spectra in Figures 7 and 8 display a computed Gaussian function (dashed curves) representing this ideal NR response.

On the Ag(111) surface the SFG signal evidenced a 3-fold dependence on ϕ, so we display spectra every 10° in the $\phi = 0-50°$ range. Over this range the NR intensity varied by more than a factor of 6, and the R component evolved through the peak, derivative, and dip forms seen in the simulated spectra of Figure 2. The solid curves in Figure 7 are the fits to eq 3, and the fits were excellent except in the wings away from the CBT resonance.

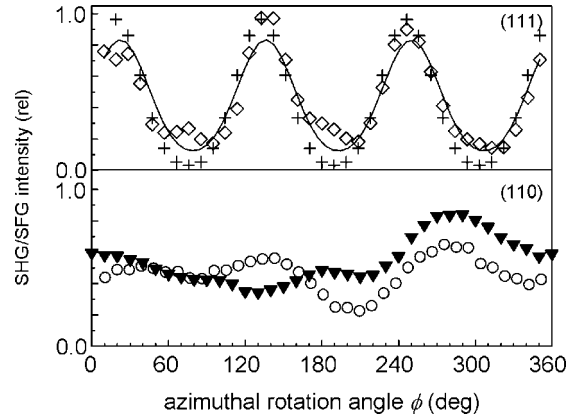

Figure 11. Variation of the SFG intensity of bare Ag surfaces with azimuthal rotation. The SFG signal is entirely NR in this case. (top) Data from Ag(111) (diamonds) is compared to SHG data from Ag(111) (crosses) reproduced from ref 28. (bottom) Data from Ag(110) (triangles) is compared to SHG data from Au(110) (circles) reproduced from ref 15.

On the Ag(110) surface the SFG signal evidenced a 2-fold dependence on ϕ, so we display spectra every 20° in the $\phi = 0-100°$ range. The NR intensity varied by a factor of about four, and the resonance appeared as a dip and a derivative shape but never as a peak.

Figures 9 and 10 show parameters extracted from these spectra. The smooth curves through the phase and $\chi^{(2)}_{NR}$ data were computed using the function,

$$f(\phi) = \{A + B\cos[n(\phi + \gamma)]\} \quad (5)$$

In Figure 9, the fit to eq 5 with $n = 3$ is excellent. The amplitudes of the R component due to the CN-stretch of the CBT adlayer were independent of ϕ. The observed variations in the R amplitudes are believed to be within experimental error.

On the Ag(110) surface the phase angle and NR amplitudes also varied with ϕ and could be fit quite accurately to eq 5 with $n = 2$. The magnitudes of the phase and NR variations were much smaller than on the Ag(111) surface. The R amplitudes were once again independent of ϕ.

A limited amount of data was acquired on bare Ag(111) and Ag(110) crystals with no adsorbed CBT SAM, in the ambient atmosphere. Figure 11 shows the SFG intensity, which is entirely NR in this case, versus ϕ for both surfaces. The Ag(111) surface NR results are quite similar to what was obtained with the CBT SAM, namely, a large variation in NR intensity with a 3-fold dependence on ϕ. The smooth curve fitting the data was again computed using eq 5 with $n = 3$. But the NR intensity variation with ϕ for the bare Ag(110) surface was quite different from the CBT-modified Ag(110) surface, and it does not evidence a 2-fold symmetry. For the sake of comparison we have plotted second-harmonic generation data obtained from other laboratories along with our SFG data in Figure 11. We compared our SFG Ag(111) to Ag(111) SHG data from Georgiadis and Richmond.[28] We could

not find any SHG azimuthal rotation data for bare Ag(110), so we compared our SFG data to Au(110) SHG data from Bilger and Pettinger.[15]

DISCUSSION

Rotational Dependence of NR Amplitudes. SFG data show that the NR amplitudes on Ag(111) and Ag(110) modified with a SAM have the expected 3-fold and 2-fold symmetries. More remarkable is the observation that NR data from a bare Ag(110) surface, shown in Figure 11, does not display 2-fold symmetry. This result shows the Ag(110) surface is unstable and undergoes a reconstructive transition under ambient conditions, likely because of oxidation, which can be reversed by binding a SAM to the surface.

Rotational Dependence of Phase. We showed that the phase ψ, that is, the relative phase between $\chi_R^{(2)}$ of the CN-stretch and $\chi_{NR}^{(2)}$ of the metal surface, varies significantly with ϕ on both Ag(111) and Ag(110) surfaces and that ψ exhibits the 3-fold or 2-fold symmetry of the crystal surface. The data in Figures 9 and 10 show that ψ appears to be a maximum when the NR amplitude is a minimum and vice versa. Although it is well-known that the phase can be varied by changing the visible pulse wavelength, the phase matching condition, the electrochemical potential, and so on, these are the first detailed measurements of how the phase changes with azimuthal orientation. We do not have any simple explanation for the observed relationship between the phase and the NR intensity. It would be useful to know if this relationship holds in a general sense, since it would simplify and improve our ability to fit orientation-dependent SFG spectra, but to know this it would be necessary to study the orientational dependence under conditions of different absolute phase, for instance while varying the visible wavelength or the electrochemical potential.

In the study by Follonier et al.,[33] the ϕ-dependence was determined by obtaining one data point at the peak of the R transition and one data point far away from the peak. In other words these authors simply subtracted the NR background away from the R signal. This procedure would work only if the phase ψ were rotation-invariant, which we see is not the case.

Rotational Dependence of R Amplitude. Using our NR suppression technique, we showed that the CN-stretch amplitude of the CBT adsorbates on both Ag(111) and Ag(110) surfaces is invariant with respect to rotation. This proves that the CN-stretch transition moment on both surfaces is parallel to the surface normal. Equation 5 shows that the transition moment, in the dipole approximation, can be factored into a dipole moment and a polarizability tensor,[42,43] so by transition moment we mean the dipole vector, which lies parallel to the C≡N axis, and it is this C≡N axis that is parallel to the surface normal.

It is interesting that we are able to obtain the rotation-invariant CN-stretch amplitude on both surfaces using conventional SFG as well. This is not a trivial task because the spectral shape and intensity vary radically with rotation. For instance in Figures 7 and 8, the actual resonance feature is nothing like a Lorentzian with constant intensity; it evolves through a series of asymmetric features ranging from a peak to a dip. It is only our ability to accurately extract the NR amplitudes and phases that allows us to make this determination. In turn this accurate extraction is related to the high signal-to-noise ratios of our spectra.

It is important to prove that we can accurately extract R amplitudes and phases in conventional SFG where both R and NR contributions combine to generate the spectrum because it is not always useful to suppress the NR signal. Determining the phase can play an important role in surface science. Measurements of the phase can be used to measure the absolute orientation of a molecule on a surface.[1,44] The ability to measure potential-dependent molecular reorientation is also based on observing a sudden inversion of the phase upon reorientation.[9,45,46]

In SFG studies of molecules on single-crystal substrates with a fixed orientation, such as electrochemical measurements, with the NR suppression technique, the choice of orientation of the crystal would have no effect on the SFG spectrum. However, the spectrum can be radically altered by orientation in conventional SFG, as illustrated in Figures 7 and 8, so researchers should consider choosing crystal orientations to simplify data analysis. The best choices would typically be azimuthal orientations where the phase $\psi = 0°$ or 180°.

ACKNOWLEDGMENT

We thank Jonathan Arambula (S. Zimmerman group) for synthesizing CBT. We thank Mauro Sardela for helpful conversations regarding X-ray crystallography and orientation of our single crystal samples. This material is based upon work supported by the National Science Foundation under awards DMR 0504038 (DDD) and CHE 0603675 (A.A.G.), and the Air Force Office of Scientific Research under award FA9550-06-1-0235 (D.D.D.).

Received for review November 4, 2008. Accepted December 9, 2008.

AC802332H